Characterization of fine precipitates evolution in post ageing treatment after friction stir processed 7075Al Alloy

P. K. Mandal[1], Jithin Devasia[2], Mebin T Kuruvila[3]

Department of Metallurgical and Materials Engineering, Amal Jyothi College of Engineering, Kanjirappally-686518, Kerala, India

Abstract—*The effect of post ageing treatment (140°C for 2h) on the microstructure and mechanical behaviour of FSPed 7075 Al alloy has been studied by Optical microscopy (OM), Field emission scanning electron microscopy (FESEM), Differential scanning calorimetry (DSC), Scanning electron microscopy (SEM), Transmission electron microscopy (TEM), and mechanical properties. Friction stir processing (FSP) is a solid-state surface modification technique to apply for cast aluminium alloys. FSP has a similar metal working principle like FSW (friction stir welding). The alloy has strong age-hardening response with scandium (Sc) inoculated Al-Zn-Mg alloy, on the other hand novelty of FSP only few studies have been carried out to the effect of post ageing treatment on the microstructure, size, morphology and fine dispersion of coherent $Al_3Sc(L1_2)$ type precipitates or ή-phases and its mechanical properties of friction stir processed 7075 Al alloy. The FSPed enhances grain boundary (GB) formation and increases suitable sites for the precipitation of nucleation in post aged 7075 Al alloy. Themechanical properties have been evaluated such as proof strength ($\sigma_{0.2}$) of 122. 9 MPa, ultimate tensile strength (σ_u) of 256. 4 MPa, ductility (δ) of 8. 6%, Vicker's hardness in stir zone of 101 HV, strain hardening exponent (n) of 1. 82, and heat input during FSPed of 2. 15 kJ/mm, respectively.*

Keywords*—*Al_3Sc and ή precipitates, FSP, mechanical properties, post aged 7075 Al alloy, TEM.

I. INTRODUCTION

The high strength Al-Zn-Mg alloy (7075 series) was widely used due to their spontaneous age-hardening ability, good corrosion resistance and excellent mechanical properties obtained through fine precipitation of a homogeneous distribution of dispersiod particles [1-3]. Further, friction stir processing (FSP) has been adapted for surface modification technology, especially for fabrication process, processing and synthesis of materials. It has great advantages including surface modification for microstructural evaluation, adjusting mechanical properties by optimizing tool design and process parameters [4, 5]. FSP can be exploited not only by controlling process parameters but also by using an Al-Zn-Mg-Sc alloy contains thermally stable precipitates or dispersoids, also can precipitate out such particles during processing thereby retarding the uncontrolled grain growth. Hence, fine-grained microstructure may be obtained by controlling the grain growth or fine distribution of Al_3Sc precipitates during FSPed plus post ageing treatment [6-8]. Ma and Mishra et al. [2005] demonstrated the possibility of achieving grains larger than 1 µm under any other processing conditions. As well, Nascimento et al. [2009], Kwon et al. [2003], and Colligan et al. [1999] insight studied on FSP technique successfully to produce fine-grained structure and surface composite of aluminium alloys. More emphasis has been given on the mechanism of dynamic recrystallization in Al-Zn-Mg-Sc alloy and the role of coherent precipitates in the formation of high temperature (450-550°C) FSPed microstructure. In addition, heat input (2. 15 kJ/mm) is the main criterion for the energy transformation during FSPed [9-11]. The characteristics of fine-grained microstructure obtained through FSP are entirely different from any other conventional severe plastic deformation (SPD) techniques. Thus, the major processing parameters are the tool rotation and traverse speed, the axial force, tile angle and the proper tool design have been well documented by several authors. The possible strengthening mechanism can be attributed to formation of fine grain and subgrain structure and dislocation distribution of the modified surface [12-14]. The objective of the present work is to characterize the precipitates in friction stir processed Al-Zn-Mg-Sc alloy then post ageing treatment at 140°C for 2h using OM, FESEM, SEM, DSC, and TEM analysis. To investigate the effects of scandium on mechanical properties of FSPed aluminium alloy after post ageing treatment (140°C for 2h).

II. EXPERIMENTAL PROCEDURE

The muffle furnace was used to melt the 7075 Al alloy, and subsequently Sc added an inoculation effect in-form of Al-2wt % Sc master alloy through foundry route. The melt was carried out in a mild steel mould (200×90×24mm^3) and melting temperature fixed at 780°C. The pieces of aluminium around 3. 5 kgs, kept into a graphite crucible, and its put into a muffle furnace and heated upon 2. 5h until fully melt it. Then, pieces of Al-2wt. %Sc master alloy added in proportion of Sc (generally 50% recovery) into liquid bath and kept for another 30 mins for grain refinement with the carefully adjusting the fading. Then the red hot crucible was taken out from the furnace, soon Mg and Zn were added in liquid bath gradually with carefully. Slag removed from the top of the liquid bath and it was poured into metallic mould quickly. The hot mould immediately put into the water bath for faster cooling. The size of cast platewas obtained of 150×90×8 mm^3 from main coupon. The cast metal had been analyzed by ICP-AES (inductively coupled plasma atomic emission spectroscopy) and AAS (atomic absorption spectroscopy) methods and the following composition is given in weight percentage of 7075 Al alloy: Zn(5. 95%), Mg(2. 90%), Sc(0. 45%), Si(0. 10%), Fe(0. 10%), and balance of Al. While, total Zn and Mg content is 8. 85% and Zn to Mg ratio of 2:1 and Sc content 0. 45% (hypoeutectic) as shown Figure 1(a). The cast plate was preferred for solution treatment at 465^{o}C for 1h then followed by immediately quenching in water to room temperature is called T_4heat treatment. After completing the T_4 heat treatment, the same specimens were preferred for artificial ageing at 120^{o}C, 140^{o}C, and 180^{o}C for 14heach slot, respectively. This ageing kinetics has been evaluated through Vicker's hardness (FIE VM50 PC) measurements with 10 kgs. load and 15s dwell time. Each time six indentations were taken quickly on specific sample which carried out from the heating furnace and obtained average value for plotting ageing time vs. Vicker's hardness as shown in Figure 8(a-b). The T_4plate was preferred for double-pass FSP with fixed parameters are 1000 rpm, 70 mm/min traverse speed and specified tool design, then its post aged at 140^{o}C for 2h. It is clear that post ageing treatment conducted after completion of double-pass FSPed plate. Then, the samples were picked up from SZ (stir zone) and preferred for characterizations such as OM, FESEM, SEM, DSC, TEM, and mechanical testing. Samples for optical metallography were cut into small pieces for cold mounting then polished by emery papers from course to finer grades and followed by velvet cloth polishing with alumina powder slurry to obtain mirror finish. The FESEM with EDS analysis (QUANTA 200F, 30kV) was determined for GB segregations of experimental samples. The DSC (EXSTAR TG/DTA 6300) run was carried out of experimental samples for revealing semi-solid state precipitation and dissolution reactions by using a nitrogen atmosphere and a constant heating rate of 10^{o}C/min till 650^{o}C. The polished samples were cleaned by water then dried and etched in Keller's reagent (1ml HF + 1. 5ml HCl + 2. 5ml HNO_3 + 95ml H_2O) for optical microscopy. An optical microscope (LEICA DMI 5000M) was used to obtain microstructure images. TEM with SAD studies were performed using a Techai G^2 20 S-TWIN at 200kV. The TEM thin foil (80 to 100 µm) specimens were prepared through polishing by fine emery papers and subsequently through conventional twin-jet electropolishing technique using a 30%HNO_3 + 70%CH_3OH solution at -20^{o}C and 20V. After electropolishing samples (3 mm diameter and contain center hole) have preserved in vacuumdesiccator for TEM analysis. A vertical milling machine was used for surface modification of cast aluminium plate by FSP. The FSP machine consists of 3 H. P. motor mounted on top with option for 8 variable spindle speeds. The spindle speed selection was done by shifting the rubber belt to the desire groove of the four-step cone-pulleys. A hydraulic power pack controlled the movement of a semi-automatic adjustable working table. A constant axial compressive force of 15 kN was fixed before start the FSP machine and all process parameters are shown in Table 1. The processing plate (150×90×8 mm^3) had fixed on the working table with the proper fixer as shown in Figure 1(b) and subsequently a tool configuration as shown in Figure 1(c), a macrostructure of double-pass FSPed plate (Figure 1. d), a macrostructure of double-pass FSPed as showing of stir zone (Figure 1. e), and a bunch of tensile test samples as shown in Figure 1(f), respectively. The tensile samples were picked up from SZ of double-pass FSPed as shown in Figure 1(d) and Figure 1(f). It has to mention that the tool design is the most important parameter of the FSP. The tool made of heat treated martensitic stainless steel (211 HV) with cylindrical shape of shoulder and oval shape of pin tip. The tool has three main functions likely to (i) transform the applied load to the work piece, (ii) heat is generated by friction between the tool shoulder and work piece, and by the plastic deformation of the work piece, and (iii) stirring and mixing the material around it. The tool was rotated clockwise direction at the speed of 1000 rotations per min with the rotating pin inserted into the work plate. The rotating tool was then traversed in the X-axis direction perpendicular to the Y-axis direction of the work plate at a constant speed of 70 mm/min. The tool rotation Z-axis was held perpendicularly to the work plate. All FSP experiments were carried out through the double-pass and only 35% deviation in between two passes with the same direction during processing. The nugget zone or stir zone created during processing in middle place of working plate with adjacent right side and left side is called advancing side and retreating side, respectively. After FSPed, all plates were preferred for post ageing treatment at 140^{o}C for 2h in muffle furnace with controlled temperature. Then, the processed plate preferred for machining along the SZ to preparation for tensile samples (ASTM: E8/E8M-11) [15]. The tensile testing was carried out at a cross head speed of 1 mm/min in a Universal Testing Machine (UTM) (25 kN, H25, K-S, UK) in room temperature. The averages of five samples were tested for each case for evaluating of tensile properties and the results are shown in Table 2.

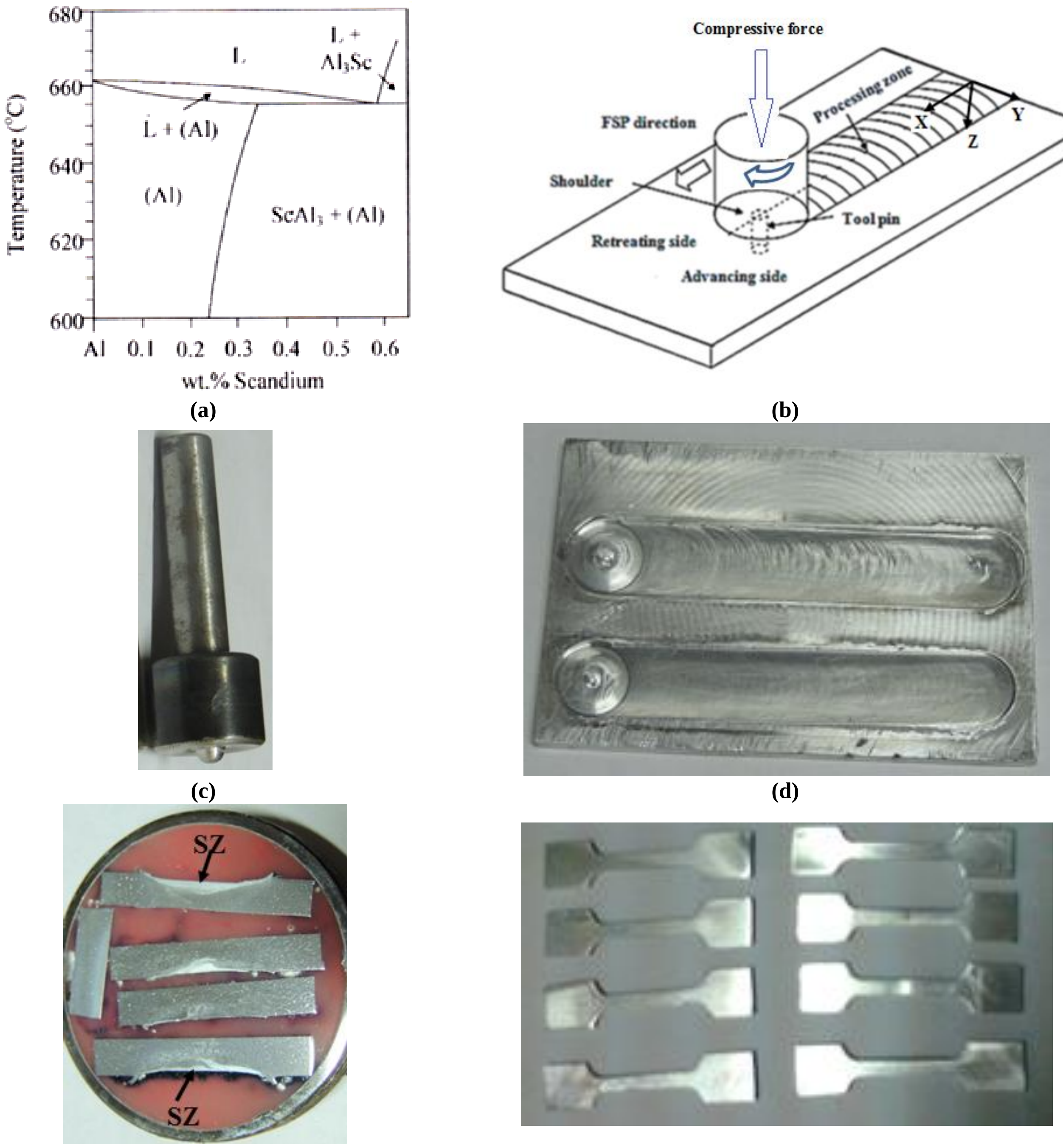

FIGURE 1: (a) The Al-Sc equilibrium phase diagram, (b) Schematic diagram of double-pass FSPed set-up (plate size:150×90×8mm^3), (c) Tool configuration, (d) Double-pass FSPed plate (each impression contain double-passFSP), (e) A bunch of macrostructures of double-pass FSPed as showing of stir zone (SZ), (f) A bunch of tensile test samples were collected from stir zone (SZ).

TABLE 1
PROCESSING PARAMETERS OF DOUBLE-PASS FSP$_{ED}$.

FSP parameters and the tool design						
Tool rotation speed(rpm)	**Work piece travel speed (mm/min)**	**Friction pressure (up-setting force) (kN)**	**Pin angle(^{o})**	**Pin root dia. and ht. (mm)**	**No. of passes**	**Plate dimensions**
1000	70	15	2. 5	5. 0, 3. 5	two	150×90×8 mm^3

III. RESULTS AND DISCUSSION

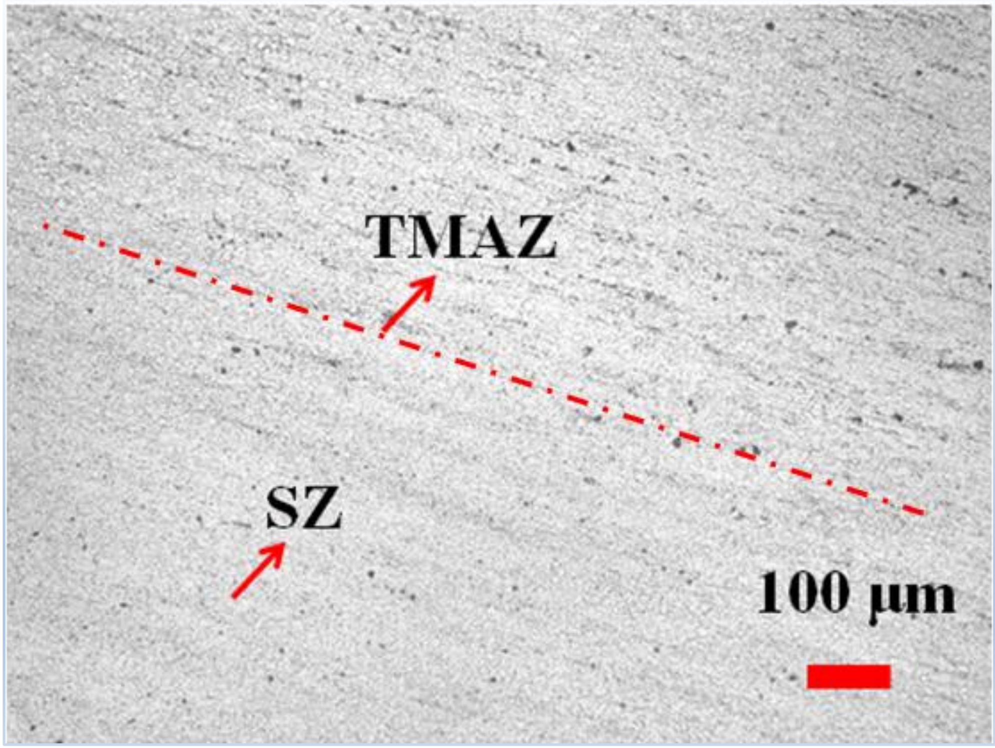

FIGURE 2: Optical micrograph of 7075 Al alloy at T_4+FSPed+Post-aged at 140°C for 2h condition. (1000 rpm and 70 mm/min)

The strength of the fine-grain aluminium alloy after FSPed from SZ can be calculated from the Hall-Patch relationship:$\sigma_y = \sigma_0 + \frac{k}{\sqrt{d}}$, where σ_y is the yield strength (0. 2% proof strength) as 143. 6 MPa, σ_0 is the friction strength, d is the grain size as 5. 31±1. 0 µm, and k (0. 22 MPa√m) is a constant for a particular material. The grain size measured by Image J software, and 0. 2% proof strength as experimental value is 143. 6 MPa (Table 2), then from the above equationσ_0 is calculated as 143. 5 MPa, it seems both of the strengths are almost same values [16, 17]. It has to mention that the increasing strength as a result of finer grains have to more number of grain boundaries in SZ after FSPed plus post aged 140°C for 2h. There are significant improvements of mechanical properties have realized through only a double-pass of FSPed. The deformedalloy in the SZ experiences adequately high temperatures (450-500°C) leading to dynamic recrystallization occurs by nucleation of very fine grains at the boundaries of the severely deformed grains in SZ. According to Jata et al. [2000] suggested that the low angle boundaries at the initial stage of parent metal are replaced by the high angle boundaries in SZ by continuous rotation of the original low angle boundaries during FSPed [18-20]. Many other researchers have been reported that the fraction of high angle grain boundaries (85-90%)is also responsible for formation of the fine and equiaxed grains produced by FSPed aluminium alloys. This high-volume fraction of high angle grain boundaries can encourage grain boundary sliding, which is estimated as the leading deformation mechanism for higher ductility and superplasticity [21, 22]. It is generally believed that achieving fine-grained sizes using FSPed is easier in this alloy that contain large number of second phase particles as η-$MgZn_2$ and numerous dispersoids as Al_3Sc in matrix. These precipitates have different interface energy that can improve the tensile properties by orientation and the post ageing treatment. Also, these particles can restrict grain growth due to their pinning effect can play the major role in grain size evolution in FSPed alloy. It is also able to calculate the heat input of 2. 15 kJ/mm during FSPed at fixed parameters as shown Table 1. Figure 2 shows optical microstructure of FSPed aluminium alloy exhibited clearly two different regions such a TMAZ which average grain size of 6. 96±2. 1 µm corresponding created several black spots average size of 10. 09±2. 1 µm, similarly SZ average grain size of 5. 31±1. 0 µm corresponding created several black spots average size of 3. 42±1. 62 µm, respectively. It has to conclude that theseblack spots generated due to Zn vaporization effect during FSPed and its deleterious effects decrease mechanical properties mainly for large size of black spots and several hair line cracks generated due to torsional effects of rotating tool in TMAZ in matrix [23, 24]. Figure 3shows the FESEM with EDX analysis exhibited several white spots mainly for Al_3Sc agglomeration and $Al_2Zn_3Mg_3$ phases with ample impurities (Fe+Si=6. 89 wt. %) content as well as Sc content of 2. 89 wt. % in the matrix. Figure 4 shows the DSC curve of alloy. There are five peaksin the curve, which are marked by letters A, B, C, D, and E, respectively.

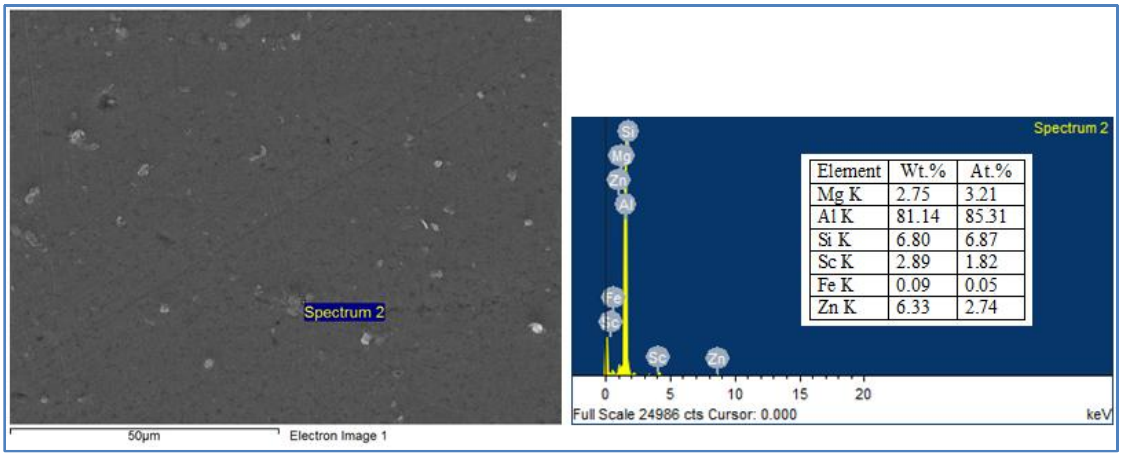

FIGURE 3: FESEM micrograph with EDX analysis of 7075 Al alloy at T_4+FSPed+ Post-aged at 140°C for 2h. (1000 rpm and 70 mm/min)

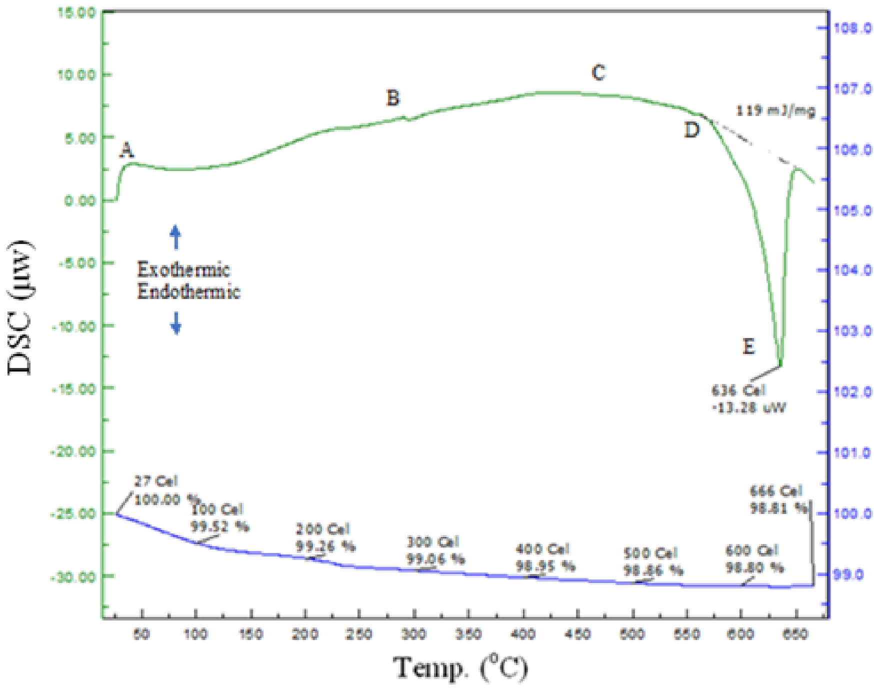

FIGURE 4: DSC analysis (heating rate 10°C/min) of 7075 Al alloy at T_4+FSP+Post-aged at 140°C for 2h. (1000 rpm and 70 mm/min)

The first peak indicates at the A point of exothermic reaction occur at around 25-30°C, which may refer for GP zones formation in matrix of alloy. The second peak indicates at the B point little deflection of endothermic reaction occur at around 285-295°C, which may refer initial phases are (GP zones, ή-metastable phases) dissolve in matrix during DSC run at 10°C/min. The third peak indicates at the C point of exothermic reaction occur at around 560-570°C, which may refer for reprecipitation of metastable phases of ή, η and Al_3Sc particles and formation of high volume fraction of the precipitates, but it has offered hardening effect till D point (endothermic reaction) in the DSC curve. The alloy is prone of endothermic reaction occur at 636°C, which may refer for completely dissolved of all hardening phases and coarsening effect of Al_3Sc particles in matrix [25, 26]. Figure 5(a) shows TEM micrograph with the SAD analysis of T_6 aluminium alloy revealed a large number of coherent secondary Al_3Sc particles (marked by red arrows and size 43. 38±10. 23 nm) of fine precipitates are distributed homogeneously in matrix. It is clearly visible at the grain boundary regions for high magnification (100 nm) of T_6 aluminium alloy (Figure 5. b). Besides the spots of Al_3Sc particles there are some fine precipitates for ή phases in the matrix. These coherent Al_3Sc particles (33. 81±6. 58 nm) have a good thermal stability and drastic anticrystallization effect. It can be seen that ageing strengthening effect of alloy is very strong. Initial stage of ageing, the strength of alloy increases rapidly then the peak can be achieved at 140°C for 6h ageing time. Therefore, Al_3Sc particles and ή phases are the main strengthening precipitates in peak-aged aluminium alloy.

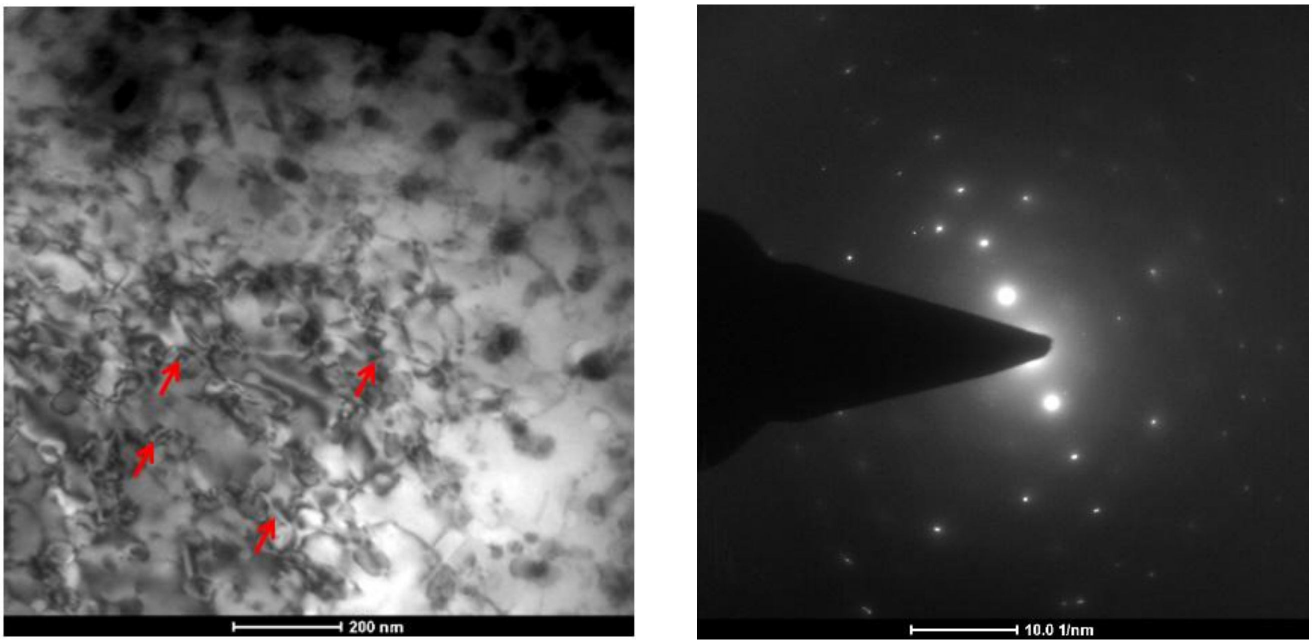

(a)

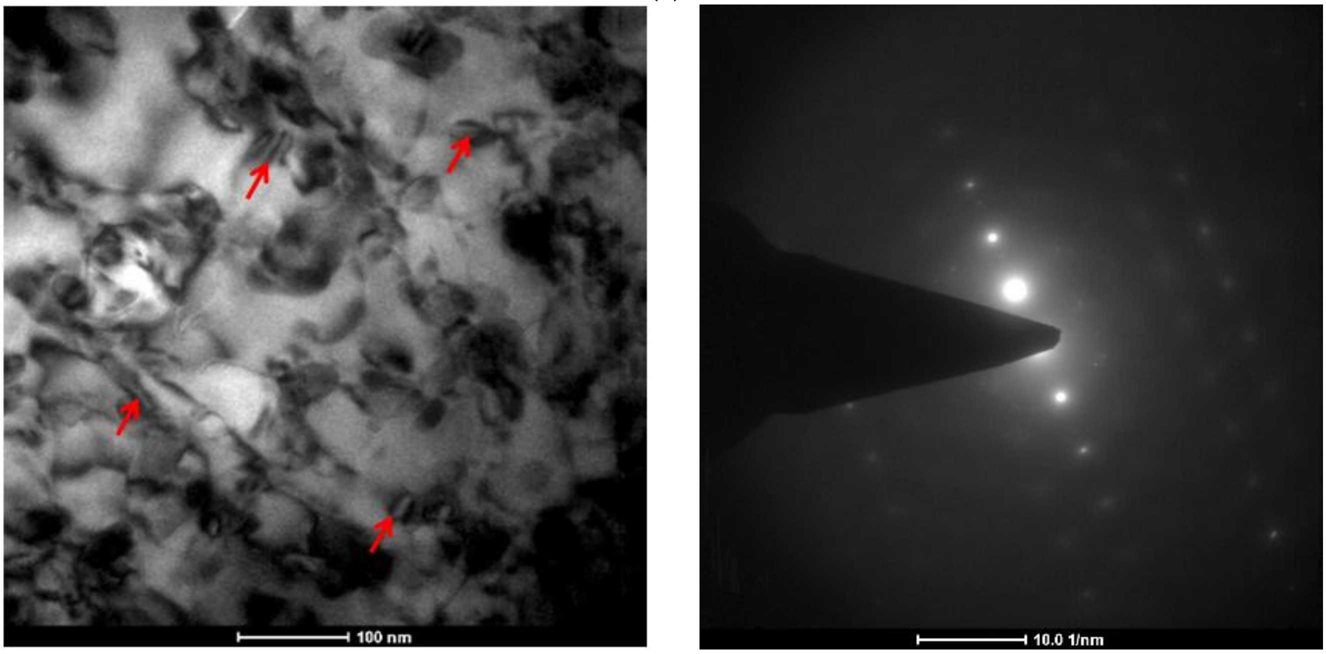

(b)

FIGURE 5: TEM micrographs with SAD patterns of 7075 Al alloy aged at 140°C for 6h (T_6): (a) at low magnification (200 nm), (b) at high magnification (100 nm).

Figure 6(a-b) shows TEM micrographs with the SAD analysis of aluminium alloy exhibited fine homogeneous precipitates with narrow zone of PFZ (precipitation free zone) and fine precipitates embedded on the grain boundary (GB) in the matrix. Mostlytwo types of precipitated particlesare dominated likely to GBP (grain boundary precipitates) of Al_3Sc type on the grain boundary and needle shape ppt (precipitates) of ή-type in the matrix. According to the micrographs of TEM analysis, the mixture of GP zones and ή-type (71. 68±9. 44 nm) and Al_3Sctype are dominant precipitates of the alloyin this post-ageing state. So, the small spherical precipitates are mainly GP (I, II) zones (15. 04±3. 30 nm) and elongated or needle shape ppt (precipitates) are the ή-type (52. 32±16. 52 nm) and cauliflower shape is Al_3Sc type (33. 43±11. 02 nm) in the matrix (Figure 6. b). The GBP of the studied alloy is form about 24. 93±5. 1 nm thick with 54. 32±16. 28 nm in length and exist in the PFZ (173. 15±7. 36 nm) at the grain boundary discontinuously (Figure 6. a). The TEM micrographs observation clearly indicated that the during FSPed plus post ageing can precipitate the nanometer-sized precipitates (GP zones, ή, $MgZn_2$ and Al_3Sc) have the strong precipitation strengthening for the alloy [27-29].

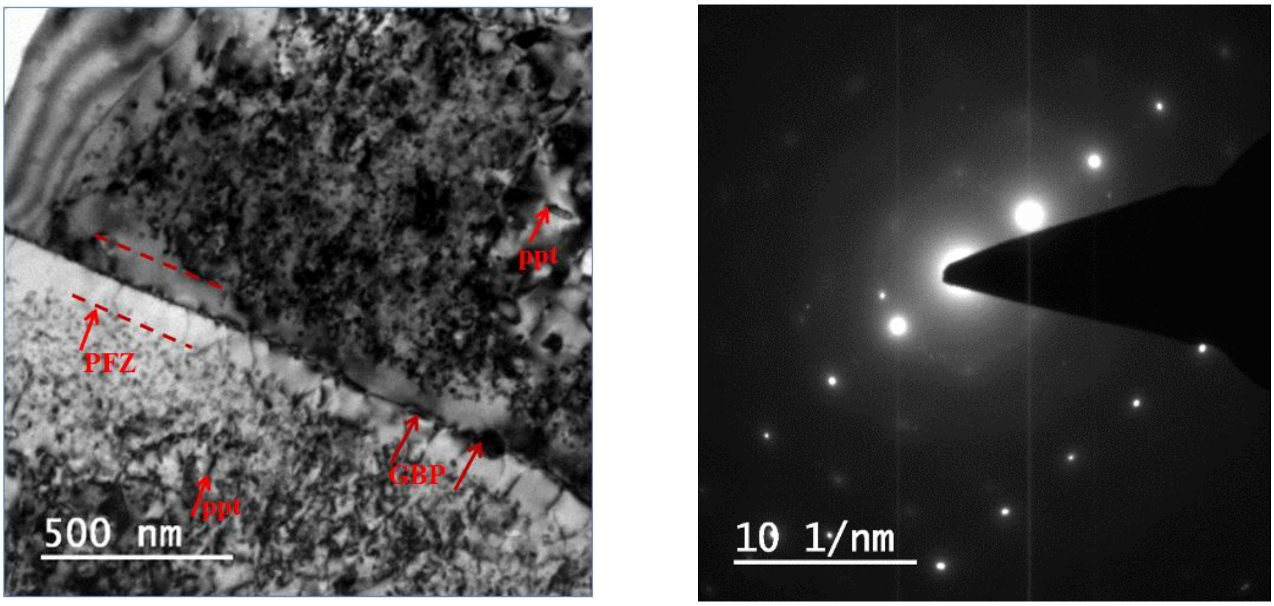

(a)

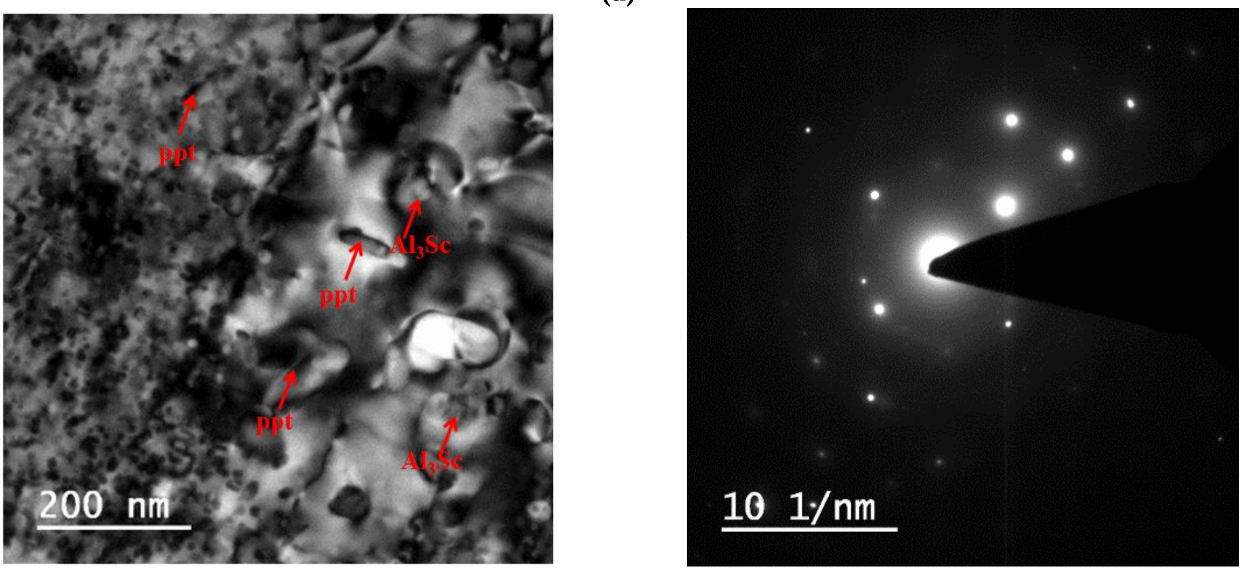

(b)

FIGURE 6: TEM micrographs with SAD patterns of 7075 Al alloy (T_4+FSP+Post-aged at 140^{o}C for 2h): (a) at low magnification (500 nm), (b) at high magnification (200 nm). (1000 rpm and70 mm/min).

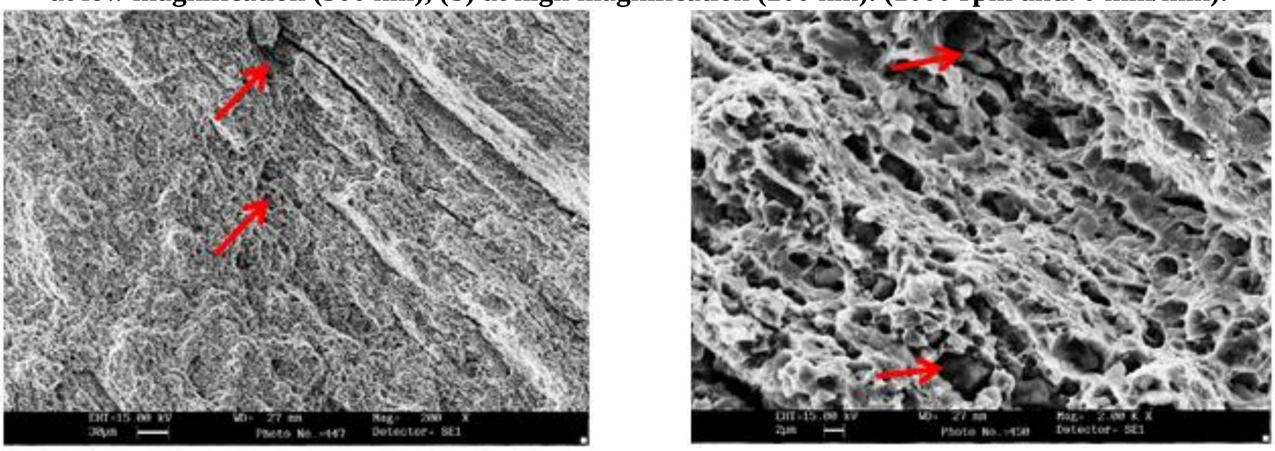

(a) **(b)**

FIGURE 7: SEM tensile fractographsof 7075 Al alloy (T_4+FSP+Post-aged at 140^{o}C for 2h): (a) at low magnification (200X), (b) at high magnification (2000X). (1000 rpm and 70 mm/min)

Figure 7 shows SEM fractograph at different magnifications exhibited mainly ductile mode of fractures propagation taking place upon transgranular manner in matrix. In the low magnification (200X) fractograph shows crack is originated from dip notch like hole (indicated by red arrows) propagating further with branches throughout the matrix. In Figure 6(b) shows the TEM analysis indicated agglomeration of coarse precipitates, defects like Zn vaporization are main causes of failure. In the high magnification (2000X) fractograph shows clear indication of many crack propagation points due to coarse precipitates (indicated by red arrows) like Al_3Sc or $Al_2Mg_3Zn_3$(T) agglomeration lead to crack extension to forward in transgranular manner and results to formation of ridge like segments in the matrix [30-32].

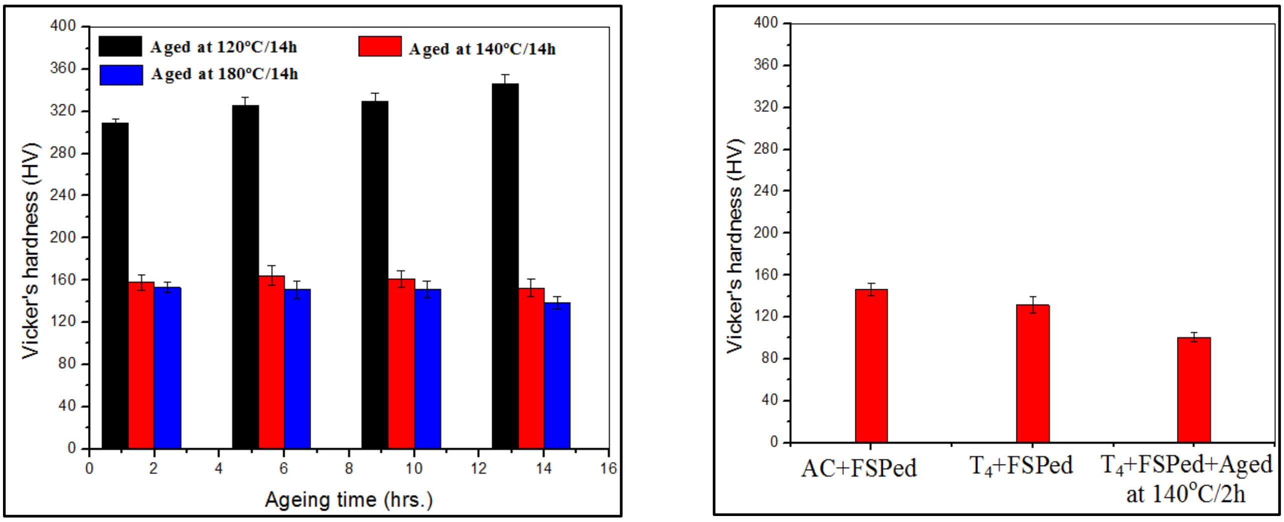

(a) **(b)**

FIGURE 8: The Vicker's hardness bar diagrams are exhibited hardening effect at different conditions: (a) after different ageing treatments, and (b) after different FSPed conditions. (1000 rpm and 70 mm/min)

Figure 8(a) shows illustration of Vicker's hardness bar diagrams revealed hardening effect after ageing treatments at 120 to 180^{o}C for 14h of solution treated (T_4) aluminium alloy. When aged at 120^{o}C for 14h, the alloy exhibits maximum age-hardening effect nearly two times more than any other ageing treatment conditions throughout the process. Mainly two reasons have to dominate for formation of high volume fraction of GP zones and acceleration of age-hardening effects due to minor Sc addition and their responsibility for early formation of ή-phaseof 7075 Al alloy. The increase of ageing time beyond the peak ageing time causes the conversion of semi coherent precipitates (ή) to incoherent equilibrium precipitates (η) and also dissolution of GP zones and coarsening of Al_3Sc type particles. Mostly precipitates are losing the coherency, become coarsen and lightly distributed and they are easily by-passed by dislocation. When aged at 140^{o}C for 14h, the alloy exhibits lowage-hardening effect perhaps due to less density of hardening precipitates (ή) and coarsening of Al_3Sc particles. When aged at 180^{o}C for 14h, the alloy exhibits minimum age-hardening effect perhaps due to overaged precipitates (η) which are incoherent in the matrix, larger interparticle spacing and coarsening of Al_3Sc particles in the grain result in more reduction of strength [33, 34]. The effect of processing parameters on the surface macrohardness (10 kg. load) of Sc added aluminium alloy with FSPed plus different pre-heat treatment and post heat treatment conditions as shown in Figure 8(b). As a result, the hardness was enhanced with uniform distribution of hardening particles of η and Al_3Sc after FSPed in matrix. In some of cases, hardness profile showed a general softening and reduction of hardness due to high heat input for high rotational speed in spite of smaller grain size. The result means that the hardness distribution has not combined with the Hall-Patch relationship. According to the characteristics of the microstructure, the major contributions to hardness of the modified layer exposed by FSPed are fine grains and the Orowan strengthening and dislocation density due to the dispersoid particles. This significant hardness improvement can be attributed by controlling the grain size and heat input through optimum tool rotation and travelling speed. Generally, the enhanced strength found in FSPed aluminium alloy is most likely caused by recrystallized grains, residual stress due to the shoulder compression, precipitation hardening and ή, Al_3Sc additions into the soft matrix, where thermal mismatch occurs between hard particles and soft matrix. Specially, in the case of 3 segment of Figure 8(b) curve's hardness drop sharply perhaps for dissolution of precipitates or coherency loss due to high angle grain boundaries and high heat input (2. 15 kJ/mm) after post ageing treatment. Table 2 shows the results of mechanical properties of aluminium alloy after FSPed plus low temperature post ageing treatment led to the increases the proof strength(143. 6 MPa) and ultimate tensile strength (256. 4 MPa) due to precipitation strengthening, while the simultaneous increase in ductility (8. 6%) and strain hardening exponent (n) of 1. 82 obtained from logarithmic true stress-true strain curve indicate high value for good toughness (K_{IC} = 32. 8 MPa√m) after post ageing treatment is a rare phenomenon [35-37]. These together increases of ductility and strength can be attributed to concurrent incidence of precipitation with internal stress relaxation. In other words, when hardening by ageing dominates over the softening by relaxation of internal stress, an enhancementin both the strength and ductility of the FSPed alloy is possible. Furthermore, as observed from the TEM analysis (Figure 6) shows the new location of secondary phases and dispersoids at the interior grain lead to the less strain and stress localization contributing to an enhancement of ductility. This location of the precipitate due to post ageing treatment at 140^{o}C for 2h can be explained through two possible theories such as during heat treatment some dislocation walls can disappear, thus leaving many precipitates in the cell interiors. Another, the motion of dislocations existence due to the high gradient of dislocation density from walls to interior of grains and it's displacing the precipitates to interior of grains. As well, heat ratio is 14. 29 for given FSP parameters and actual heat input calculated as 2. 15 kJ/mm indicates better strength and ductility after low temperature post ageing treatment of aluminum alloy [38-40].

TABLE 2
RESULTS OF MECHANICAL PROPERTIES HAVE BEEN TABULATED AFTER T_4+FSPed+AGED AT 140^{o}C FOR 2h of Al ALLOY.

7075 Al alloy	Mechanical properties				
	0. 2% Proof strength ($\sigma_{0.2}$) in MPa	Ultimate tensile strength (σ_u) in MPa	%El (δ)	Strain hardening exponent (n)	Heat ratio (tool rotation speed/traverse speed)
	143. 6	256. 4	8. 6	1. 82	14. 29

IV. CONCLUSION

In this study, the following conclusions have been summarized below:

1) With minor Sc addition peak of ageing effect achieved earlier for high strength Al-Zn-Mg alloy.
2) After aged at 120^{o}C for 14h, the alloy exhibits maximum age-hardening effect due to formation of high volume fraction of GP zones as well as minor Sc addition and their responsibility for early formation of ή-phase of 7075 Al alloy.
3) FSP is a novel surface modification technique and resulted in substantial grain refinement with numerous commercial applications of 7075 Al alloy. During FSP of aluminium alloy the dispersoids and strengthening particles in the matrix are distributed uniformly throughout the SZ region due to the stirring action of the tool.
4) The optical micrograph revealed very fine grains (5. 31±1. 0 µm) in SZ as well as TMAZ (6. 96±2. 1 µm) region, but several black spots due to the Zn vaporization and creation of hair line cracks for torsional effects in the TMAZ. Therefore, the SZ comprises very fine grains primarily due to severe plastic deformation (SPD) and dynamic recrystallization mechanism.
5) The FESEM micrograph indicated as several white spots which have Sc content of 2. 89 wt. % and Si+Fe of 6. 89 wt. % in major portion of impurities intend to diminish the strength and ductility of FSPed Al alloy.
6) DSC thermogram indicated some distinct exothermic peaks at around 60^{o}C for formation of GP zones and go on exhibiting anti-recrystallization effects or high thermal stability means thermal strength upto 600^{o}C then softening tendency come for endothermic reaction due to dissolution of hardening phases and coarsening effects of Al_3Sc particles at around 636^{o}C.
7) The TEM micrographs have been represented as low magnification and for high magnification of studied alloy. The micrograph revealed (500 nm) very fine precipitates (e. g. Al_3Sc and $MgZn_2$) with dislocation tangles and seems high angle grain boundaries are dominated in matrix. Also, distinct grain boundary has around 54. 32±16. 28 nm width and PFZ size around 173. 15±7. 36 nmin the matrix. Other micrograph (200 nm) revealed fine precipitates as well as some coarse particles (agglomeration Al_3Sc particles or T phases) in the matrix.
8) The overall strengthening is associated with the fine grain strengthening, sub-grain and precipitation strengthening by Al_3Sc particles and $MgZn_2$ precipitates. Moreover, mixture of fine and coarse type coherent spherical Al_3Sc particles appears after T_4+FSP+Aged at 140^{o}C for 2h.

ACKNOWLEDGEMENTS

The authors are express their sincere gratitude for given opportunity of research works at the Department of Metallurgical and Materials Engineering in Indian Institute of Technology Roorkee (IITR), Uttarakhand, India.

REFERENCES

[1] Y. Deng, Z. Yin, K. Zhao, J. Duan, Z. He, "Effects of Sc and Zrmicroalloying additions on the microstructure and mechanical properties of new Al-Zn-Mg alloys", Journal of Alloys and Compounds, 530 (2012) 71-80.

[2] L-M. Wu, M. Seyring, M. Rettenmayr, W-H. Wang, "Characterization of precipitate evolution in an artificially aged Al-Zn-Mg-Sc-Zr alloy", Materials Science and Engineering A, 527 (2010) 1068-1073.

[3] H. Loffler, I. Kovacs, J. Lendvai, " Review Decomposition processes in Al-Zn-Mg alloys", Journal of Materials Science, 18 (1983) 2215-2240.

[4] M-H. Ku, F-Y. Hung, T-S. Lui, L-H. Chen, W-T. Chiang, "Microstructural Effects of Zn/Mg Ratio and Post Heat Treatment on Tensile Properties of Friction Stirred Process (FSP) Al-xZn-yMg Alloys", Materials Transactions, Vol. 53, 5(2012) 995-1001.

[5] Z. Y. Ma, "Friction Stir Processing Technology: A Review", Metallurgical and Materials Transactions A, Vol. 39A (March 2008) 642-658.

[6] K. Li, X. Liu, Y. Zhao, "Research Status and prospect of Friction Stir Processing Technology", Coatings, 9, 129 (2019) 1-14.

[7] A. Goloborodko, T. Ito, X. Yun, Y. Motohashi, G. Itoh, "Friction Stir Welding of a Commercial 7075-T_6 Aluminium Alloy: Grain Refinement, Thermal Stability and Tensile Properties", Materials Transactions, Vol. 45, 8(2004) 2503-2508.

[8] A. Kurt, I. Uygur, E. Cete, "Surface Modification of aluminium by friction stir processing", Journal of Materials Processing Technology, 211(2011) 313-317.

[9] M. M. El Rayes, E. A. El Danaf, M. S. Soliman, "High-temperature deformation and enhanced ductility of friction stir processed-7010 Aluminium Alloy", Materials and Design, 32 (2011) 1916-1922.

[10] R. Kumar, K. Singh, S. Pandey, "Process forces and heat input as function of process parameters in AA5083 friction stir welds", Transactions of Nonferrous Metals Society of China, 22(2012) 288-298.

[11] H. Chen, B. Yang, "Effect of Precipitations on Microstructures and Mechanical Properties of Nanostructured Al-Zn-Mg-Cu Alloy", Materials Transactions, Vol. 49, 12(2008) 2912-2915.

[12] A. D. Isadare, B. Aremo, M. O. Adeoye, O. J. Olawale, M. D. Shittu, "Effect of Heat Treatment on Some Mechanical Properties of 7075 Aluminium Alloy", Materials Transactions, 16(1), (2013) 190-194.

[13] K. Wang, F. C. Liu, Z. Y. Ma, F. C. Zhang, "Realization of exceptionally high elongation at high strain rate in a friction stir processed Al-Zn-Mg-Cu alloy with presence of liquid phase", ScriptaMaterialia, 64(2011) 572-575.

[14] J. Chen, L. Zhen, S. Yang, W. Shao, S. Dai, "Investigation of precipitation behavior and related hardening in AA 7055 aluminium alloy", Materials Science and Engineering A, 500(2009) 34-42.

[15] G. R. Cui, Z. Y. Ma, S. X. Li, "The origin of non-uniform microstructure and its effects on the mechanical properties of a friction stir processed Al-Mg alloy", ActaMaterialia, 57(2009) 5718-5729.

[16] X. Feng, H. Lu, S. S. Babu, 'Effect of grain size refinement and precipitation reactions on strengthening in friction stir processed Al-Cu alloys', ScriptaMaterialia, 65(2011) 1057-1060.

[17] Z. Ahmad, "The Properties and Application of Scandium-Reinforced Aluminium", Journal of The Minerals, Metals and Materials Society, Vol. 55, Issue 2, 530(Feb. 2003) 35-39.

[18] J-Q. Su, T. W. Nelson, C. J. Sterling, 'Microstructure evolution during FSW/FSP of high strength aluminium alloys', Materials Science and Engineering A, 405(2005) 277-286.

[19] Y. Deng, R. Ye, G. Xu, J. Yang, Q. Pan, B. Peng, X. Cao, Y. Duan, Y. Wang, L. Lu, Z. Yin, "Corrosion behaviour and mechanism of new aerospace Al-Zn-Mg alloy friction stir welded joints and the effects of secondary $Al_3Sc_xZr_{1-x}$ nanoparticles", Corrosion Science, 90(2015) 359-374.

[20] V. J. Arulmoni, R. S. Mishra, "Friction Stir Processing of Aluminium alloys for Defense Applications", International Journal of Advance Research and Innovation, Vol. 2, Issue 2 (2014) 337-341.

[21] M. Shamanian, H. Mostaan, M. Safari, 'Friction stir modification of GTA 7075-T_6 Al alloy weld joints: EBSD study and microstructural evolutions', Archives of Civil and Mechanical Engineering, 17(2017) 574-585.

[22] A. Kumar, A. K. Mukhopadhyay, K. S. Prasad, "Superplastic behaviour of Al-Zn-Mg-Cu-Zr alloy AA7010 containing Sc", Materials Science and Engineering A, 527(2010) 854-857.

[23] L-M. Wu, W-H. Wang, Y-F. Hsu, S. Trong, "Effects of homogenization treatment on recrystallization behaviour and dispersoid distribution in an Al-Zn-Mg-Sc-Zr alloy", Journal of Alloys and Compounds, 456(2008) 163-169.

[24] T. Hu, K. Ma, T. D. Topping, J. M. Schoenung, E. J. Lavernia, "Precipitation phenomena in an ultrafine-grained Al alloy", ActaMaterialia, 61(2013) 2163-2178.

[25] N. Afify, A-F. Gaber, G. Abbady, "Fine Scale Precipitates in Al-Zn-Mg Alloys after Various Aging Temperatures", Materials Sciences and Applications, 2(2011) 427-434.

[26] O. N. Senkov, S. V. Senkova, M. R. Shagiev, "Effect of Sc on Aging Kinetics in a Direct Chill Cast Al-Zn-Mg-Cu Alloy", Metallurgical and Materials Transactions A, Vol. 39A (May 2008) 1034-1053.

[27] S. Gholami, E. Emadoddin, M. Tajally, E. Borhani, "Friction stir processing of 7075 Al alloy and subsequent aging treatment", Transactions of Nonferrous Metals Society of China, 25(2015) 2847-2855.

[28] N. Kumar, R. S. Mishra, Ultrafine-Grained Al-Mg-Sc Alloy via Friction-Stir Processing, Metallurgical and Materials Transactions A, Vol. 44A, (Feb. 2013)934-945.

[29] P. K. Mandal, J. Felix Kumar, "Investigation of precipitation Behaviour and Related Microstructural and Mechanical properties after FSP of Aluminium Alloy", International Advanced Journal of Engineering Research, Vol. 2, Issue 11 (November 2019) 15-19.

[30] Z. Chen, Y. Mo, Z. Nie, "Effect of Zn Content on the Microstructure and Properties of Super-High Strength Al-Zn-Mg-Cu Alloys", Metallurgical and Materials Transactions A, Vol. 44A, (Aug. 2013) 3910-3920.

[31] J. Ma, D. Yan, L. Rong, Y. Li, "Effect of Sc addition on microstructure and mechanical properties of 1460 alloy", Progress in Natural Science: Materials International, 24(2014) 13-18.

[32] X. Ju, F. Zhang, Z. Chen, G. Ji, M. Wang, Y. Wu, S. Zhong, H. Wang, "Microstructure of Multi-Pass Friction-Stir-Processed Al-Zn-Mg-Cu Alloys Reinforced by Nano-Sized TiB_2 Particles and the Effect of T_6 Heat Treatment", Metals, 7, 530(2017) 1-15.

[33] S. Hirosawa, T. Hamaoka, Z. Horita, S. Lee, K. Matsuda, D. Terada, "Methods for Designing Concurrently Strengthened Severely Deformed Age-Hardenable Aluminium Alloys by Ultrafine-Grained and Precipitation Hardenings", Metallurgical and Materials Transactions A, Vol. 44A, (Aug. 2013) 3921-3933.

[34] M. R. Clinch, S. J. Harris, W. Hepples, N. J. H. Holroyd, M. J. Lawday, B. Noble, "Influence of Zinc to Magnesium Ratio and Total Solute Content on the Strength and Toughness of 7xxx series Alloys", Materials Science Forum, Vols. 519-521(2006) 339-344.

[35] H. Zhenbo, Y. Zhimin, L. Sen, D. Ying, S. Baochuan, Z. Xiang, "Preparation, microstructure and properties of Al-Zn-Mg-Sc alloy tubes", Journal of Rare Earths, Vol. 28, No. 4, (August 2010) 641-646.

[36] M. Vratnica, Z. Cvijovic, N. Radovic, "THE EFFECT OF COMPOSITIONAL VARIATIONS ON THE FRACTURE TOUGHNESS OF 7000 Al-ALLOYS", Materials and Technology, 42, 5(2008) 191-196.

[37] A. C. Reddy, S. S. Rajan, "Influence of ageing, inclusions and voids on ductility fracture mechanism in commercial Al-alloys", Bulletin of Material Science, Vol. 28, No. 1, (February 2005) 75-79.

[38] S. Dadbakhsh, A. K. Taheri, C. W. Smith, "Strengthening study on 6082 Al alloy combination of aging treatment and ECAP process", Materials Science and Engineering A, 527(2010) 4758-4766.

[39] P. K. Mandal, "Study on hardening mechanisms in aluminium alloys", International Journal of Engineering Research and Applications, Vol. 4, Issue 1, Part-6 (January 2016)91-97.

[40] G. M. Ludtka, D. E. Laughlin, "The Influence of Microstructure and Strength on the Fracture Mode and Toughness of 7XXX Series Aluminium Alloys", Metallurgical Transactions A, Vol. 13A (March 1982) 411-425.